HHS Public Access

Author manuscript

J Rheumatol. Author manuscript; available in PMC 2018 November 18.

Published in final edited form as:

J Rheumatol. 2014 January ; 41(1): 65–74. doi:10.3899/jrheum.111476.

Upregulation of ANK Protein Expression in Joint Tissue in Calcium Pyrophosphate Dihydrate Crystal Deposition Disease

Miwa Uzuki, MD, PhD[#],
Department of Pathology, Division of Leading Pathophysiology, Iwate Medical University, School of Medicine, and Division of Rheumatology, Medical College of Wisconsin

Takashi Sawai, MD, PhD,
Department of Pathology, Division of Leading Pathophysiology, Iwate Medical University, School of Medicine

Lawrence M. Ryan, MD,
Division of Rheumatology, Medical College of Wisconsin

Ann K. Rosenthal, MD, and
Division of Rheumatology, Medical College of Wisconsin

Ikuko Masuda, MD, PhD[#]
Division of Rheumatology, Medical College of Wisconsin, and Institute of Rheumatology, Tokyo Women's Medical University.

[#] These authors contributed equally to this work.

Abstract

Objective—Accumulation of excess extracellular inorganic pyrophosphate leads to calcium pyrophosphate dihydrate (CPPD) crystal formation in articular cartilage. CPPD crystal formation occurs near morphologically abnormal chondrocytes resembling hypertrophic chondrocytes. The ANK protein was recently implicated as an important factor in the transport of intracellular inorganic pyrophosphate across the cell membrane. We characterized ANK in joint tissues from patients with and without CPPD deposition and correlated the presence of ANK with markers of chondrocyte hypertrophy.

Methods—Articular tissues were obtained from 24 patients with CPPD crystal deposition disease, 11 patients with osteoarthritis (OA) without crystals, and 6 controls. We determined the number of ANK-positive cells in joint tissues using immunohistochemistry and *in situ* hybridization, and correlated ANK positivity with markers of chondrocyte hypertrophy including Runx2, type X collagen, osteopontin (OPN), and osteocalcin (OCN).

Results.—ANK was detected in synoviocytes, chondrocytes, osteoblasts, and osteocytes. ANK was seen extracellularly only in the matrix of cartilage and meniscus. The number of ANK-positive cells was significantly higher in CPPD than in OA or normal joint tissues. The amount and intensity of ANK immunoreactivity reached maximum levels in the large chondrocytes around

Address correspondence to Dr. M. Uzuki, Department of Pathology, Division of Leading Pathophysiology, Iwate Medical University, School of Medicine, 2-1-1 Nishitokuta, Yahaba-cho, Shiwa-gun, Iwate, 028-3694, Japan, muzuki@iwate-med.ac.jp.

crystal deposits. ANK was similarly distributed to and significantly correlated with Runx2, type X collagen, OPN, and OCN.

Conclusion.—ANK levels were higher in articular tissues from patients with CPPD deposition. ANK was concentrated around crystal deposits and correlated with markers of chondrocyte hypertrophy. These findings support a role for ANK in CPPD crystal formation in cartilage. (First Release Dec 1 2013; J Rheumatol 2014;41:65–74; doi:10.3899/jrheum.m476)

Keywords

ANK; CALCIUM PYROPHOSPHATE DIHYDRATE; CARTILAGE; PATHOLOGY; IMMUNOHISTOCHEMISTRY; IN SITU HYBRIDIZATION

Osteoarthritis (OA) affects 50% of people over age 65[1] and is often associated with pathologic mineralization of affected cartilage[2]. For example, calcium pyrophosphate dihydrate (CPPD) crystal deposits occur in 20% of OA joints at the time of joint replacement[3]. Although the role that calcium-containing crystals play in OA is not fully understood, there is ample evidence to suggest these crystals are active participants in joint damage. *In vitro,* calcium-containing crystals initiate or amplify cartilage destruction by stimulating mitogenesis of synovial lining cells and inducing the synthesis and secretion of proteases and cytokines from synovial cells and chondrocytes[4]. The presence of calcium-containing crystals in joint fluids may predict increased severity of joint damage and more rapid joint destruction[5]. Theoretically, prevention or reversal of crystal deposition should stop the progression of joint degeneration.

CPPD crystals are typically found in hyaline and fibrocartilage and at areas of chondroid metaplasia in synovium, tendon, and ligament in affected joints. Histologic studies demonstrate extracellular crystals in the pericellular space around morphologically abnormal chondrocytes with abnormal safranin-O positivity[6]. It has been postulated that these chondrocytes are similar to the hypertrophic chondrocytes responsible for matrix mineralization in growth plate cartilage[7,8], and the matrix around CPPD crystal deposits contains increased levels of products of hypertrophic chondrocytes such as osteopontin (OPN)[9]. While many factors influence CPPD crystal deposition, excess accumulation of inorganic pyrophosphate (PPi), the anionic component of the CPPD crystal, has been the best studied[10,11]. Synovial fluid PPi levels are elevated in patients with CPPD crystal deposition[12]. PPi levels correlate with the severity of radiographically evident cartilage degeneration[13]. Extracellular inorganic pyrophosphate (ePPi) elaboration is greater in cultured chondrocytes from CPPD-diseased cartilage than from healthy controls and individuals with OA. Previous studies have shown that articular cartilage is the primary source of articular ePPi, and articular chondrocytes are unusual in their ability to spontaneously elaborate significant amounts of ePPi.

PPi is a byproduct of multiple intracellular synthetic reactions, but it cannot diffuse across biomembranes to reach the extracellular environment where CPPD crystals are formed. To participate in extracellular crystal formation, PPi must be actively transported across the biomembrane or formed *de novo* outside the cell by ectoenzymes that break down adenosine-5’-triphosphate (ATP) and other nucleoside triphosphates. Animal models and *in*

vitro studies support both mechanisms of ePPi production in chondrocytes. Ho, *et al* demonstrated that the transmembrane protein ANK was an important factor in PPi transport[14]. ANK is a multipass transmembrane protein that may control movement of intracellular inorganic pyrophosphate (iPPi) across the cell membrane, or possibly movement of precursors of PPi such as ATP[15]. Ho, *et al* reported that the *ank* gene mutation in mouse fibroblasts increases iPPi concentration and reduces ePPi concentration. Overexpression of wild-type ANK in mutant *ank/ank* mouse fibroblasts reversed the alterations in ePPi and iPPi levels, indicating an important role for ANK in regulating PPi trafficking[14]. Subsequently, mutations of *ANKH,* the human homolog of the *ank* gene, were documented in patients with familial and sporadic CPPD[16,17].

In our present study, we sought to elucidate the possible biological roles of ANK in CPPD disease by characterizing the expression of ANK in joint tissues of patients with and without CPPD deposition, and correlating ANK immunoreactivity with the presence of markers of chondrocyte hypertrophy.

MATERIALS AND METHODS

Tissue samples.

All tissue specimens were obtained from hospitals affiliated with Iwate Medical University Hospital, Morioka, Tohoku University Hospital, Sendai, and Kumamoto University Hospital, Kumamoto, Japan, from 1995 to 2007. Informed consent was obtained from each patient. The study was carried out in accordance with the Declaration of Helsinki (1989) of the World Medical Association, and was approved by the ethics committees of the hospitals involved. Samples of hyaline cartilage, meniscus, synovium, and bone were obtained at the time of joint replacement or arthroscopic synovectomy from 24 patients with OA with CPPD crystals (20 women, 4 men, age 70.4 ± 7.6 yrs), who met the criteria of Ryan and McCarty for CPPD (1985)[18], and 11 patients with OA without CPPD (10 women, 1 man, age 69.3 ± 10.3 yrs). Similar tissues from 6 healthy subjects obtained after surgeries for trauma or amputation (3 women, 3 men, age 44.3 ± 17.0) were used as controls. Tissues were dissected into 125–1000 mm^3 pieces and fixed in 4% (W/V) paraformaldehyde dissolved in phosphate buffered saline (PBS) solution for 2 h at room temperature, before embedding in paraffin. Sections 2-μm thick were cut and mounted on glass slides coated with poly-L-lysine or silane. For each sample, serial tissue sections were stained with H&E and safranin-O to assess the degree of cartilage degeneration and histological findings.

Immunohistochemistry.

Immunostaining of paraffin-embedded sections was performed by the modified ABC method using an Avidin-Biotin-Complex (ABC) kit (Vector Laboratories Inc.). After deparaffinization, the sections were treated with 0.3% (V/V) hydrogen peroxide in methanol for 30 min at room temperature to block endogenous peroxidase activity. After washing in PBS, the slides were covered with 10% (V/V) normal goat serum (NGS) in PBS for 40 min at room temperature to block the nonspecific binding of second antibody (goat antirabbit IgG antibody) reaction. The excess NGS was removed, and sections were covered with antiserum (Ab1 and Ab3) to mouse ANK (provided by Dr. D. Kingsley, Stanford University

School of Medicine)[14] and incubated overnight (18 h) at 4°C. Anti-ANK antibodies were generated against peptides containing amino acids 118 to 130 (Ab1) and 477 to 492 (Ab3) of murine ANK and were used at a 1:1000 dilution. We determined the most suitable dilution after titration 1:100, 1:200, 1:400, 1:500, 1:1000, and 1:2000. After washing with PBS, sections were covered with the second antibody [goat biotinylated-antirabbit IgG antibody (Vector Laboratories Inc.)] and incubated for 40 min at room temperature. After washing in PBS, sections were covered with ABC for 40 min at room temperature and rinsed in PBS. Antigenic sites were demonstrated by reacting the sections with a 3, 3' diaminobenzidine tetrahydrochloride (Sigma Chemical Co.) for 7 min. The sections were then counterstained with methyl green, dehydrated in ethanol, cleared in xylene, and mounted. As a negative control, nonimmune rabbit IgG (final concentration of IgG 200 ng/ml) was used in place of the ANK antibody. The total number of cells and numbers of ANK-positive cells were counted in 20 randomly chosen high-power fields (HPF; ×400) and the results were expressed as the mean percentage of ANK-positive cells. ANK positivity in the extracellular matrix was measured by calculating the positive area of matrix/total area of matrix × 100 (%). Staining results were very similar between ANK antibodies Ab1 and Ab3 (data not shown). Our result was compatible with that of Ho, *et al*[14]. Background staining was a little stronger in Ab1 than Ab3. We adopted antibody against Ab3 epitope for counting the positive cells.

Quantification of ANK and other markers in serial tissue sections.

To correlate the presence of ANK and markers of hypertrophy, 4 serial tissue sections were treated with ANK antiserum or other antibodies, respectively. Runx2 (Santa Cruz, goat polyclonal), type X collagen (LSL, rabbit polyclonal), OPN (Chemicon, rabbit polyclonal), and osteocalcin (OCN; R&D systems, mouse monoclonal) were used as markers for hypertrophic chondrocytes. In all specimens that were processed for immunohistochemistry, ANK, Runx2, and type X collagen, OCN-positive, and OPN-positive cells were counted in at least 20 different microscopic fields chosen randomly from each section. Results were expressed as the positive ratio [positive cells/number of total cells] × 100 (%)] at a magnification of ×400 (HPF). We compared the distribution of the ANK-positive cells with that of Runx2, type X collagen, OPN, and OCN-positive cells in the same fields of the serial tissue sections.

Preparation of RNA probes for mRNA in situ hybridization.

Total RNA from cultured chondrocytes of the patients with CPPD was extracted by the acidified guanidinium isothiocyanate method, using TRIzol reagent (Life Technologies). Samples of total RNA (0.2 μg for cartilage extract) were reverse-transcribed into complementary DNA (cDNA) in the presence of 50 pM oligo (dT)12–18 primer (Life Technologies), 10 units of ribo- nuclease inhibitor (Amersham), 10 × reverse transcriptase (RT) buffer, deoxyribonucleoside triphosphate (dNTP mixture; 5 mM each dNTP), and reverse transcriptase (Omniscript RT kit, Qiagen Inc.) for 60 min at 37°C. Amplification of generated cDNA was performed in a GeneAmp PCR System 2400 thermocycler (Perkin-Elmer Bio Systems) using Platinum PCR Supermix (Life Technologies). The gene-specific primer pairs were as follows: ANK sense 5'-TGG GAT GTG CCT CAA TCT CA-3', antisense 5'-CAC AGA GTT CTG CAA AGG CAA-3; Runx2 sense 5'-CCA CCT CTG

ACT TCT GCC TC-3', antisense 5'-GAC TGG CGG GGT GTA AGT AA-3'; Type X collagen sense 5'-GCC TGA GGG TTTTAT AAA GG-3', antisense 5'-TTA GCT CTG TGG GGT GTA C-3'; OCN sense 5'-CAT GAG AGC CCT CAC ACT CC-3', antisense 5'-CAG CAG AGC GAC ACC CTA GAC C-3'; OPN sense 5'-AGG CTG ATT CTG GAA GTT CTG AGG-3', antisense 5'-ACT CCT CGC TTT CCA TGT GTG AGG-3'; GAPDH, sense 5'-GGT GAA GGT CGG AGT CAA CG-3', antisense 5'-CAA AGT TGT CAT GGA TGA CC-3'. Cycling measurements were as follows: for ANK, 32 cycles of 95°C for 30 s, 58°C for 30 s, and 72°C for 30 s; for Runx2, 35 cycles of 95°C for 30 s, 58°C for 30 s, and 72°C for 60 s; for type X collagen, 35 cycles of 95°C for 30 s, 60°C for 30 s, and 72°C for 60 s; for OPN, 35 cycles of 95°C for 30 s, 58°C for 30 s, and 72°C for 60 s; for OCN, 35 cycles of 95°C for 30 s, 60°C for 30 s, and 72°C for 60 s; for GAPDH, 25 cycles of 95°C for 30 s, 55°C for 30 s, and 72°C for 30 s. An additional elongation step at 72°C for 7 min was included. Transcripts were analyzed by 1.2% agarose/Tris-acetate-EDTA gel electrophoresis and visualized with SYBR GREEN-I (Sigma) using image scanner Storm (Molecular Dynamics). The expected transcript sizes were 600 bp for ANK, 180 bp for Runx2, 428 bp for type X collagen, 533 bp for OPN, 331 bp for OCN, and 496 bp for GAPDH. The sequence of each PCR product was confirmed by dideoxy chain-termination sequencing after subcloning the PCR product into Topo TA cloning vector (pCR II-TOPO; Invitrogen). The plasmid DNA-containing target gene was linearized by using XhoI to prepare the antisense strand and Hind III for the sense strand. The probes were labeled with digoxigenin-11-UTP by using a digoxigenin (DIG) RNA-labeling kit (SP6/T7; Roche Diagnostics GmbH, Roche Applied Science)[19,20].

In situ hybridization.

Hybridization procedures in our study were performed as described[21] using a slightly modified nonradioactive *in situ* hybridization technique with DIG-labeled RNA probes[22,23,24,25]. Paraffin-embedded tissues were cut into 2-μm-thin sections and mounted onto silane-coated slides. They were deparaffinized and treated with pepsin solution (2.5 mg/ml; Phoenix BioTechnologies Inc.) for 5 min at 95°C followed by 0.05N hydrochloric acid for 10 min. The sections were then postfixed with 4% paraformaldehyde in PBS for 20 min and treated with glycine (2 mg/ml) in PBS twice for 3 min each. After washing with PBS, the samples were acetylated with a freshly prepared mixture of 0.25% acetic anhydride in triethanolamine buffer for 10 min. The DIG-labeled RNA probes (250 ng/ml) in a formamide-free diluent (Brigati probe diluent; Phoenix BioTechnologies Inc.) were placed on the slides and covered with Parafilm M. Hybridization was performed in a humidified chamber on a waterbath for 18 h at 45°C. For the negative control, sense probes were used. After hybridization and removal of Parafilm M by immersing the slides in 2× standard saline-citrate buffer (SSC; 2 × SSC is 0.15M NaCl, 0.015M trisodium citrate pH7.0) for 1 h at room temperature, sections were washed in 2 × SSC 3 times at room temperature, 0.5 × SSC once at 45°C, and 0.1 × SSC 3 times at 45°C for 10 min each. The DIG-labeled probes were visualized following the protocol described in the DIG nucleic acid detection kit (Roche Diagnostics GmbH, Roche Applied Science). The slides were incubated with alkaline phosphatase (ALP)-conjugated anti-DIG antibody for 1 h at room temperature. Hybridization products were visualized as blue purple using nitro-blue tetrazolium chloride/5-bromo-4-chloro-3'-indolyphosphate p-toluidine salt. The slides were

counterstained with methyl green and coverslipped with glycerol/PBS for microscopic examination. Quantification of positivity was performed as above.

Statistical analysis.

Data are represented as means ± SD, and differences between groups were analyzed by the nonparametric Mann-Whitney U test, Student's paired t test, and Pearson correlation coefficients. Differences were considered statistically significant at $p < 0.05$.

RESULTS

ANK immunoreactivity in articular tissues.

ANK-immuno-reactive cells were observed in all CPPD tissues examined, including synovial cells (Figure 1a), chondrocytes (Figure 1b and g), osteoblasts (Figure 1c), CPPD crystal deposits themselves (Figure 1d and g), and the extracellular matrix around CPPD crystals (Figure 1e and g). No significant staining was detected in negative control (Figure 1h). ANK protein in the cell cytoplasm displayed a granular staining pattern (Figure 2a) in chondrocytes of nondegenerated cartilage, and a linear pattern (Figure 2b) was observed on cell membranes of hypertrophic chondrocytes in damaged cartilage. In nondegenerated tissues, synovial cells and chondrocytes showed granular staining pattern as in Figure 2a. In degenerated tissues, synovial cells and chondrocytes showed linear staining pattern on cell membranes as in Figure 2b. We did not find these differences on osteoblasts. ANK protein was particularly prevalent in the hypertrophic chondrocytes with safranin-O positive inclusions around CPPD crystal deposits (Figure 3). The number of ANK-positive cells in cartilage, meniscus, and synovium from OA patients with no crystals and controls were fewer than in OA with CPPD (Table 1 and Figure 4). The percentage of ANK-positive cells in CPPD cartilage (64.1 ± 25.1%) was significantly greater than that in cartilage from OA or trauma patients (22.4 ± 10.2%; $p < 0.001$). The percentages of ANK-positive cells in CPPD meniscus (84.4 ± 21.2 %) and synovium (60.3 ± 30.5 %) were also significantly greater than those in OA or trauma meniscus (20.8 ± 7.3%) and synovium (3.2 ± 2.2%; $p < 0.001$). The number of positive cells includes cytoplasmic type and/or membrane type. Table 1 shows the summary of the data. The number of ANK-positive cells increased in parallel with the amount of crystal deposition in the synovium, cartilage, or meniscus (data not shown). The relative immunointensity of ANK-positive cells in CPPD-containing specimens was also greater than that of tissues from patients without CPPD deposits.

ANK staining patterns were different among the 3 groups of patients (Figure 4a, b, and c). In CPPD-containing tissues, more positive cells with each pattern were seen than in OA or trauma. The linear pattern of staining on cell membranes was particularly common in tissues with CPPD deposition (6-fold higher in cartilage, 42-fold higher in meniscus, 233-fold higher in synovium). The number of ANK-positive cells in articular tissues from patients with trauma (Figure 4d, e, and f) and OA without CPPD (Figure 4g, h, and i) is fewer than CPPD: the presence of ANK protein can be seen in chondrocytes (Figure 4d and g), meniscus cells (Figure 4e and h), and synovial cells (Figure 4f and i).

We also examined the local distribution of ANK-positive cells in different areas of meniscus and cartilage. In the inner zone of meniscus, which was also more frequently degenerated, the number of ANK-positive cells was greater than that of the outer zone. Similarly, in hyaline cartilage, more ANK-positive cells were seen in the highly degenerated superficial zone than in the more intact deeper zone.

Local expression of ANK mRNA in the synovial tissue.

ANK mRNA hybridization signals were detected in the cytoplasm of synovial cells (Figure 5a), chondrocytes (Figure 3d and 5b), and osteoblasts (Figure 5c) in articular tissues from patients with CPPD-deposition disease. Negative controls showed no signal. The distribution of ANK mRNA hybridization signals was similar to that of ANK immunoreactivity (Figure 3). The number of ANK mRNA hybridization-positive signals in CPPD cartilage and meniscus was significantly greater than that of OA or healthy controls (Figure 5d, e, f, and g), and the number of positive cells increased in proportion to the quantity of CPPD deposition.

Correlation of ANK-positive cells with markers of chondrocyte hypertrophy.

We also determined whether ANK positivity correlated with markers of chondrocyte hypertrophy using the same fields in serial tissue sections. The distribution of ANK-positive cells (Figure 6a) correlated with the presence of Runx2 (Figure 6b), type X collagen (Figure 6c), OPN (Figure 6d), and OCN (Figure 6e)-positive cells in articular tissue. In addition, the number of ANK-positive cells significantly correlated with that of Runx2, type X collagen, OPN, and OCN-positive cells ($r = 0.49$, $r = 0.62$, $r = 0.77$, $r = 0.78$, respectively; Figure 6f-i).

DISCUSSION

ANK is a multipass membrane protein implicated in CPPD deposition disease through its actions as a PPi transporter or a regulator of PPi transport across the cell membrane. PPi levels are a crucial determinant of mineralization in many tissues. While excess accumulation of PPi in articular tissues leads to CPPD crystal formation, PPi typically acts as a potent inhibitor of calcium phosphate crystal formation in other locations. For example, in bone, Wang, *et al* reported that blocking ANK transport activity in terminally differentiated mineralizing growth plate chondrocytes led to increases of intracellular and extracellular PPi concentrations and inhibition of calcium phosphate-associated mineralization[26].

We demonstrate here that levels of ANK protein and mRNA are increased in the articular tissues of patients with CPPD deposition compared to those with OA without CPPD crystals or normal controls. Our work supports and extends that of Hirose, *et al* who reported that basal expression of ANK mRNA was higher in cultured CPPD chondrocytes and CPPD cartilage extracts than in OA or normal cartilage[10]. In our study, the number and intensity of ANK positivity reached maximum levels in cells around deposits of CPPD crystals, suggesting a direct role of ANK in CPPD crystal formation. Similar staining patterns with *in situ* hybridization and immunohistochemistry confirm that the same cells that display ANK

protein also produce ANK. These findings strongly support previous work suggesting a functional role for ANK in CPPD crystal deposition disease. The pattern of ANK staining may reveal something about its function. In CPPD-diseased tissue, ANK-positive cells were seen not only in hyaline cartilage but also in the meniscus and in the synovial tissue around crystal deposits. This staining pattern further supports a direct role for ANK in CPPD crystal formation. Interestingly, in OA tissues, fewer cells contained ANK and the immunoreactivity was frequently confined to the cytoplasm. ANK has no known cytoplasmic function; however, it may be stored in granules ready for transport to the membrane under certain conditions. ANK was seen not only in chondrocytes but also in the extracellular matrix around CPPD crystals. Hirose, *et al* demonstrated release of ANK protein from cultured chondrocytes[10]. While a function for extracellular ANK is uncertain, the presence of this membrane protein in matrix raises the possibility that extracellular ANK is present in the chondrocyte-derived matrix vesicles that participate in CPPD crystal formation[27]. Indeed, ANK was represented in a recent proteomic analysis of human cartilage-derived matrix vesicles[28]. Alterations of the chondrocyte phenotype have been noted in both OA and in CPPD deposition disease. Chondrocytes around CPPD deposits are morpho- logically abnormal and share features with the hypertrophic chondrocytes responsible for matrix mineralization in growth plate cartilage. ANK was particularly frequently and intensely expressed in hypertrophic chondrocytes around CPPD deposits. ANK immunoreactivity was typically membrane-associated in these cells, supporting its function as a membrane transporter. ANK positivity strongly correlated with the presence of type X collagen, a commonly used marker of chondrocyte hypertrophy[3]. ANK positivity also correlated with the presence of Runx2, a transcription factor that is expressed in hypertrophic chondrocytes. Takeda, *et al* demonstrated that continuous expression of Runx2 in nonhypertrophic chondrocytes led to the development of abnormal chondrocyte hypertrophy[29]. OPN, a calcium-binding protein that regulates extracellular matrix mineralization, and OCN, a marker of mature osteoblast and bone formation, were also distributed in a similar pattern to ANK. Rosenthal, *et al* reported that OPN may play an important role in facilitating CPPD crystal formation in articular cartilage[9]. They showed that OPN stimulated ATP-induced CPPD crystal formation by chondrocytes *in vitro.* They also demonstrated the presence of OPN in the pericellular matrix of chondrocytes adjacent to CPPD deposits. The role that ANK plays in chondrocyte hypertrophy, and whether that role is a direct effect of its action on PPi levels, remains uncertain. Kirsch, *et al* reported that suppression of ANK expression led to decreased gene expression of bone markers, including ALP, OCN, and type I collagen *in vitro*[30]. ANK-overexpressing, hypertrophic, nonmineralizing growth plate chondrocytes showed increased mineralization-related gene expression of ALP, type I collagen, and OCN. Costello, *et al* showed that ANK overexpression leads to increased levels of extracellular ATP, another strong stimulant of cartilage mineralization[15]. Phosphate itself can also regulate cell phenotype[31].

Little is known about the regulation of ANK in articular tissues. In *in vitro* studies, ePPi accumulation has been shown to be regulated by growth factors, cytokines, and other bioactive mediators. Transforming growth factor-β1 (TGF-P1) remains one of the strongest known stimulants of ePPi. TGF-β1 increases ANK expression as well as ePPi production[32]. Johnson and Terkeltaub reported that upregulation of wild-type ANK in normal

chondrocytes not only raised ePPi but also directly stimulated matrix calcification and inhibited collagen and sulfated proteoglycan synthesis. In addition, upregulated ANK induced chondrocyte matrix metalloprotease-13 to promote matrix loss[33]. ANK expression and ePPi may exert deleterious effects in degenerative arthropathies beyond stimulation of calcification.

Limitations of our study included the quantitative difficulties inherent in immunostaining methods, and the lack of blinded observers. To minimize these limitations, we carefully counted the number of immunoreactive cells on photographs and averaged 20 fields for each tissue sample. The relatively large number of patients and controls also helps control for error. The inclusion of tissues from patients with endstage disease may result in bias. However, human tissues from less-severe cases are often very difficult to obtain. Lastly, the slightly younger age of the controls makes it impossible to rule out an aging effect in these findings.

Increased levels of the PPi-regulating membrane protein ANK were observed in the joint tissues of patients with CPPD disease compared to similar tissues from patients with OA and from healthy controls. ANK positivity was concentrated at regions of CPPD deposition and correlated with markers of the hypertrophic phenotype. These findings support the concept that increased ANK levels contribute to CPPD crystal formation in cartilage.

ACKNOWLEDGMENT

We thank Dr. David M. Kingsley (Stanford University School of Medicine) for kindly donating ANK-specific antibodies.

REFERENCES

1. Yelin E, Callahan LF. The economic cost and social and psychological impact of musculoskeletal conditions. National Arthritis Data Work Groups. Arthritis Rheum 1995;38:1351–62. [PubMed: 7575685]
2. Doyle DV. Tissue calcification and inflammation in osteoarthritis. J Pathol 1982;136:199–216. [PubMed: 7069525]
3. Fuerst M, Bertrand J, Lammers L, Dreier R, Echtermeyer F, Nitschke Y, et al. Calcification of articular cartilage in human osteoarthritis. Arthritis Rheum 2009;60:2694–703. [PubMed: 19714647]
4. Cheung HS, Ryan LM. Role of crystal deposition in matrix degradation In: Woessner FJ, Howell DS, eds. Joint cartilage degradation: basic and clinical aspects. New York: Marcel Dekker; 1995:209–23.
5. Nalbant S, Martinez JA, Kitumnuaypong T, Clayburne G, Sieck M, Schumacher HR, Jr. Synovial fluid features and their relations to osteoarthritis severity: new findings from sequential studies. Osteoarthritis Cartilage 2003;11:50–4. [PubMed: 12505487]
6. Ishikawa K, Masuda I, Ohira T, Yokoyama M. A histologic study of calcium pyrophosphate dihydrate crystal deposition disease. J Bone Joint Surg Am 1989;71:875–86. [PubMed: 2545720]
7. Eerola I, Salminen H, Lammi P, Lammi M, von der Mark K, Vuorio E, et al. Type X collagen, a natural component of mouse articular cartilage: association with growth, aging, and osteoarthritis. Arthritis Rheum 1998;41:1287–95. [PubMed: 9663487]
8. Masuda I, Ishikawa K, Usuku G. A histologic and immunohistochemical study of calcium pyrophosphate dihydrate crystal deposition disease. Clin Orthop Rel Res 1991;263:272–87.
9. Rosenthal AK, Gohr CM, Uzuki M, Masuda I. Osteopontin promotes pathologic mineralization in articular cartilage. Matrix Biol 2007;26:96–105. [PubMed: 17123806]

10. Hirose J, Ryan LM, Masuda I. Up-regulated expression of cartilage intermediate-layer protein and ANK in articular hyaline cartilage from patients with calcium pyrophosphate dihydrate crystal deposition disease. Arthritis Rheum 2002;46:3218–29. [PubMed: 12483726]
11. Johnson K, Terkeltaub R. Inorganic pyrophosphate (PPI) in pathologic calcification of articular cartilage. Front Biosci 2005;10:988–97. [PubMed: 15569637]
12. Rachow JW, Ryan LM, McCarty DJ, Halverson PC. Synovial fluid inorganic pyrophosphate concentration and nucleotide pyrophosphohydrolase activity in basic calcium phosphate deposition arthropathy and Milwaukee shoulder syndrome. Arthritis Rheum 1988;31:408–13. [PubMed: 2833903]
13. Rosenthal AK, Henry LA. Retinoic acid stimulates pyrophosphate elaboration by cartilage and chondrocytes. Calcif Tissue Int 1996;59:128–33. [PubMed: 8687982]
14. Ho AM, Johnson MD, Kingsley DM. Role of the mouse ank gene in control of tissue calcification and arthritis. Science 2000;289:265–70. [PubMed: 10894769]
15. Costello JC, Rosenthal AK, Kurup IV, Masuda I, Medhora M, Ryan LM. Parallel regulation of extracellular ATP and inorganic pyrophosphate: roles of growth factors, transduction modulators, and ANK. Connect Tissue Res 2011;52:139–46. [PubMed: 20604715]
16. Williams CJ, Pendleton A, Bonavita G, Reginato AJ, Hughes AE, Peariso S, et al. Mutations in the amino terminus of ANKH in two US families with calcium pyrophosphate dihydrate crystal deposition disease. Arthritis Rheum 2003;48:2627–31. [PubMed: 13130483]
17. Netter P, Bardin T, Bianchi A, Richette P, Loeuille D. The ANKH gene and familial calcium pyrophosphate dihydrate deposition disease. Joint Bone Spine 2004;71:365–8. [PubMed: 15474385]
18. Ryan LM, McCarty DJ. Calcium pyrophosphate crystal deposition disease: pseudogout, articular chondrocalcinosis In: McCarty DJ, ed. Arthritis and allied conditions: a textbook of rheumatology. 10th edition. Philadelphia: Lea & Febiger; 1985:1515–46.
19. Strehlau J, Pavlakis M, Lipman M, Shapiro M, Vasconcellos L, Harmon W, et al. Quantitative detection of immune activation transcripts as a diagnostic tool in kidney transplantation. Proc Natl Acad Sci U S A 1997;94:695–700. [PubMed: 9012847]
20. Sanger F, Nicklen S, Coulson AR. DNA sequencing with chain terminating inhibitors. Proc Natl Acad Sci U S A 1977;74:5463–7. [PubMed: 271968]
21. Hayashi M, Ninomiya Y, Parsons J, Hayashi K, Olsen BR, Trelstad RL. Differential localization of mRNAs of collagen types I and II in chick fibroblasts, chondrocytes, and corneal cells by in situ hybridization using cDNA probes. J Cell Biol 1986;102:2302–9. [PubMed: 3011812]
22. Montone KT, Brigati DJ. In situ molecular pathology: instrumentation, oligonucleotides, and viral nucleic acid detection. J Histotechnol 1994;17:195–201.
23. Felgar RE, Montone KT, Furth EE. A rapid method for detection of hepatitis C virus RNA by in situ hybridization. Mod Pathol 1996;9:696–702. [PubMed: 8782210]
24. Sasano H, Uzuki M, Sawai T, Nagura H, Matsunaga G, Kashimoto O, et al. Aromatase in human bone tissue. J Bone Miner Res 1997;12:1416–23. [PubMed: 9286757]
25. Uzuki M, Sasano H, Muramatsu Y, Totsune K, Oki Y, Takahashi K, et al. Urocortin in the synovial tissue of patients with rheumatoid arthritis. Clinical Science 2001;100:577–89. [PubMed: 11352772]
26. Wang W, Xu J, Du B, Kirsch T. Role of the progressive ankylosis gene (ank) in cartilage mineralization. Mol Cell Biol 2005; 25:312–23. [PubMed: 15601852]
27. Derfus B, Kranendonk S, Camacho N, Mandel N, Kushnaryov V, Lynch K, et al. Human osteoarthritic cartilage matrix vesicles generate both calcium pyrophosphate dihydrate and apatite in vitro. Calcif Tissue Int 1998;63:258–62. [PubMed: 9701631]
28. Rosenthal AK, Gohr CM, Ninomiya J, Wakim BT. Proteomic analysis of articular cartilage vesicles from normal and osteoarthritic cartilage. Arthritis Rheum 2011;63:401–11. [PubMed: 21279997]
29. Takeda S, Bonnamy JP, Owen MJ, Ducy P, Karsenty G. Continuous expression of Cbfa1 in nonhypertrophic chondrocytes uncovers its ability to induce hypertrophic chondrocyte differentiation and partially rescues Cbfa1-deficient mice. Genes Dev 2001;15:467–81. [PubMed: 11230154]

30. Kirsch T, Kim HJ, Winkles JA. Progressive ankylosis gene (ank) regulates osteoblast differentiation. Cells Tissues Organs 2009;189:158–62. [PubMed: 18728347]

31. Giachelli CM. The emerging role of phosphate in vascular calcification. Kidney Int 2009;75:890–7. [PubMed: 19145240]

32. Cailotto F, Bianchi A, Sebillaud S, Venkatesan N, Moulin D, Jouzeau JY, et al. Inorganic pyrophosphate generation by transforming growth factor-beta-1 is mainly dependent on ANK induction by Ras/Raf-1/extracellular signal-regulated kinase pathways in chondrocytes. Arthritis Res Ther 2007;9:R122. [PubMed: 18034874]

33. Johnson K, Terkeltaub R. Upregulated ank expression in osteoarthritis can promote both chondrocyte MMP-13 expression and calcification via chondrocyte extracellular PPi excess. Osteoarthritis Cartilage 2004;12:321–35. [PubMed: 15023384]

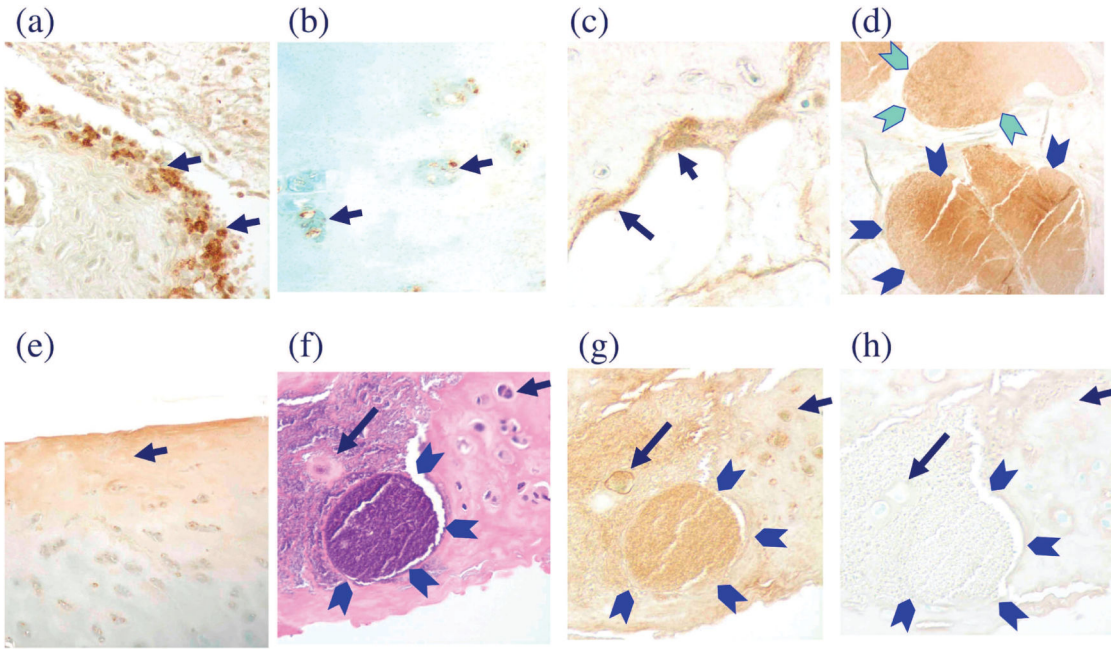

Figure 1.

Examples of ANK-positive cells in articular tissues from patients with calcium pyrophosphate dihydrate (CPPD) deposition disease. The presence of ANK protein is demonstrated by brown staining and can be seen in (a) synovial cells (arrows), (b) and (g) chondrocytes (arrows), and (c) osteoblasts (arrows). Panels (d) and (g), the crystal deposits themselves (arrowheads), and (e), extracellular matrix (arrow), also showed some staining. Serial tissue sections of a region with CPPD crystal deposition were stained with (f) H&E. Panel (g) shows ANK antibody and (h) shows nonimmune rabbit immunoglobulin. The same field is shown in each panel. No significant staining was detected in the negative control (h). Staining is particularly prominent around CPPD crystal deposits (g). Arrows show same cells in (f), (g), and (h). Arrowheads show crystal deposits in (d), (f), (g), and (h).

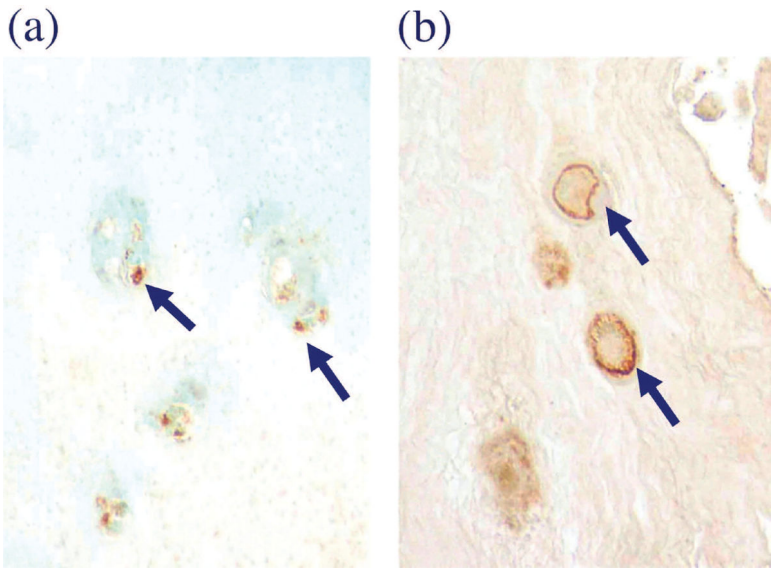

Figure 2.

The cellular distribution of ANK protein. Two different patterns of ANK staining were observed. Cytoplasmic ANK protein appeared in a granular pattern (a) in chondrocytes of nondegenerated cartilage, while ANK on cell membranes demonstrated linear staining (b) in hypertrophic chondrocytes in damaged hyaline cartilage. Arrows show positive cells.

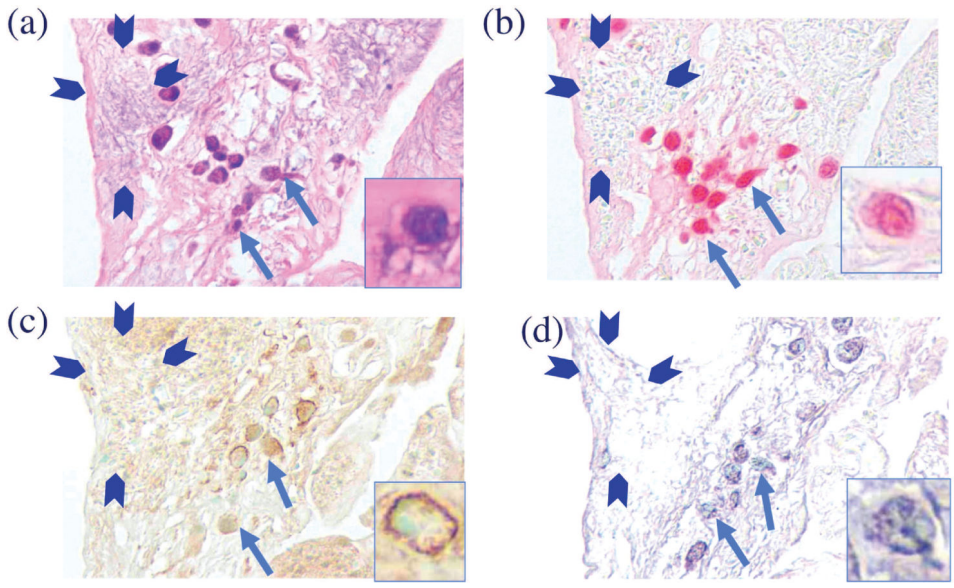

Figure 3.

ANK protein and mRNA are seen in large safranin-O-positive chondrocytes near calcium pyrophosphate dihydrate (CPPD) deposits. Tissue sections of damaged hyaline cartilage from a patient with CPPD deposition were stained with (a) H&E, (b) safranin-O, or (c) ANK antibody, or (d) underwent *in situ* hybridization for ANK mRNA. ANK-positive cells were mainly present in the hypertrophic chondrocytes with safranin-O-positive staining around crystal deposits. Inserts in each panel show hypertrophic chondrocyte. Arrows show same cluster of chondrocytes in each panel. Arrowheads show crystal deposits. Crystal was eluted from the tissue because of hydrochloric acid treatment at *in situ* hybridization reaction (d).

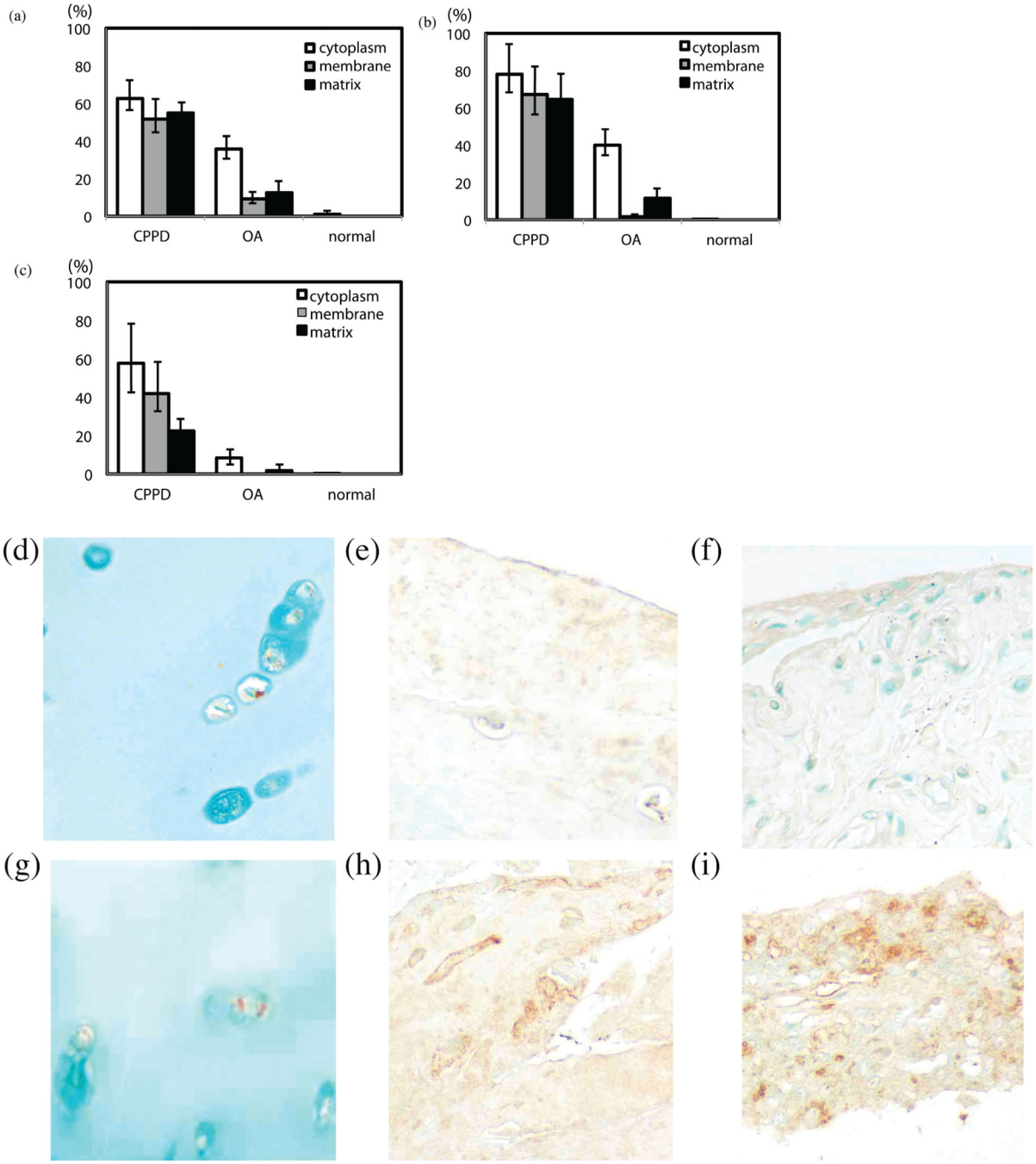

Figure 4.

More ANK-positive cells were present in tissues from patients with calcium pyrophosphate dihydrate (CPPD) disease than in tissues from patients with osteoarthritis (OA) or normal controls. We counted the number of ANK-positive cells in 20 microscope fields for each sample and noted the frequency of different staining patterns (cytoplasmic, membrane-associated, or matrix-associated). The number of ANK-positive cells in the joint tissues was significantly higher in CPPD disease than in OA or normal, particularly in cell membranes ($p < 0.001$). In CPPD, the number of positive cells with each pattern was larger than OA,

especially with the membrane pattern of distribution [6-fold higher in cartilage (a), 42-fold higher in meniscus (b), and 233-fold higher in synovium (c)]. The number of ANK-positive cells in articular tissues from patients with trauma [panels (d), (e), and (f)] and OA without CPPD [panels (g), (h), and (i)] is fewer than CPPD. The presence of ANK protein can be seen in (d) and (g) chondrocytes, (e) and (h) meniscus cells, and (f) and (i) synovial cells.

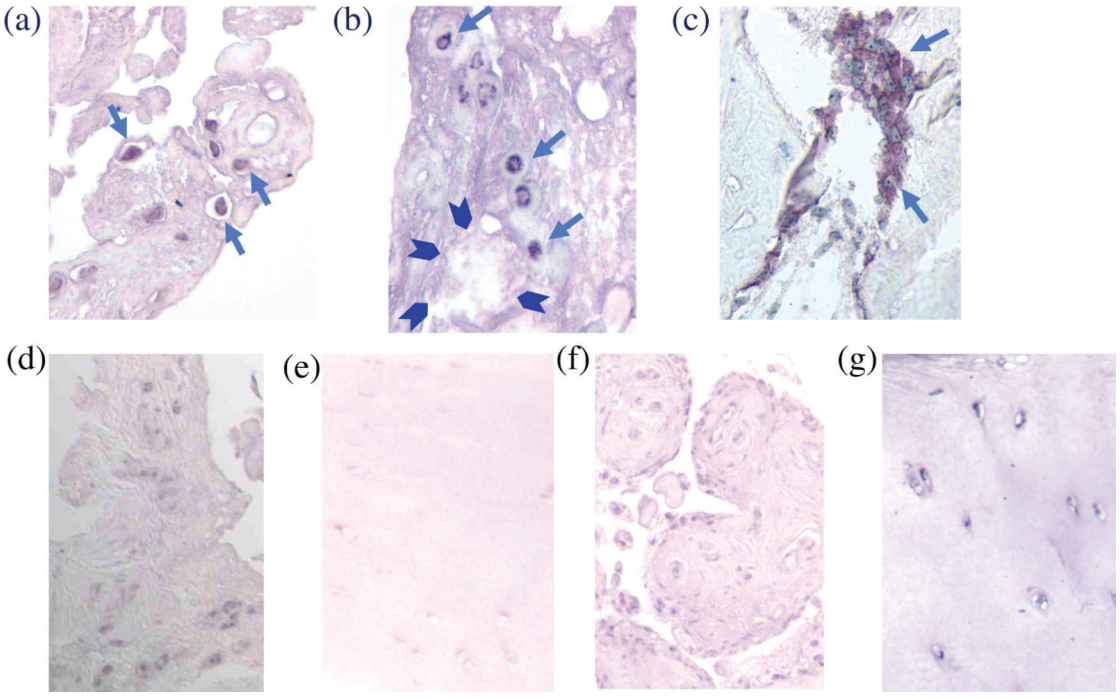

Figure 5.

ANK protein mRNA *in situ* hybridization signals. ANK mRNA hybridization signals were detected in the cytoplasm of (a) synovial cells, (b) chondrocytes, and (c) osteoblasts in articular tissues from patients with calcium pyrophosphate dihydrate (CPPD) deposition disease. The distribution of ANK mRNA hybridization signals was similar to that of ANK immunoreactivity (Figure 3). Arrows show positive cells. Arrowheads show crystal deposits in panel (b). The number of ANK mRNA hybridization-positive signals in CPPD cartilage and meniscus was significantly greater than in healthy controls [(d) and (e)] or OA without CPPD [(f) and (g)]. Panels (d) and (f) are synovial cells, and (e) and (g) are chondrocytes.

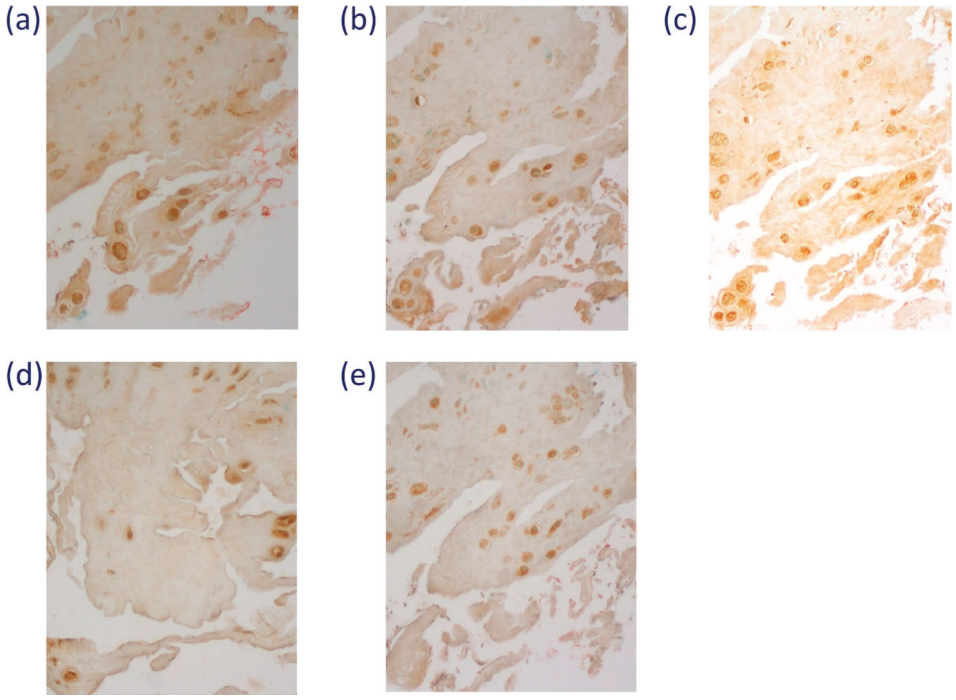

Figure 6A-E.

ANK protein is present in cells with markers of the hypertrophic phenotype. Serial tissue sections were stained with ANK antibody or antibody to a variety of markers of the hypertrophic phenotype. The distribution of (a) ANK positive cells overlapped with (b) Runx2, (c) type X collagen, (d) osteopontin (OPN), and (e) osteocalcin (OCN)-positive cells in tissue samples from patients with calcium pyrophosphate dihydrate deposition.

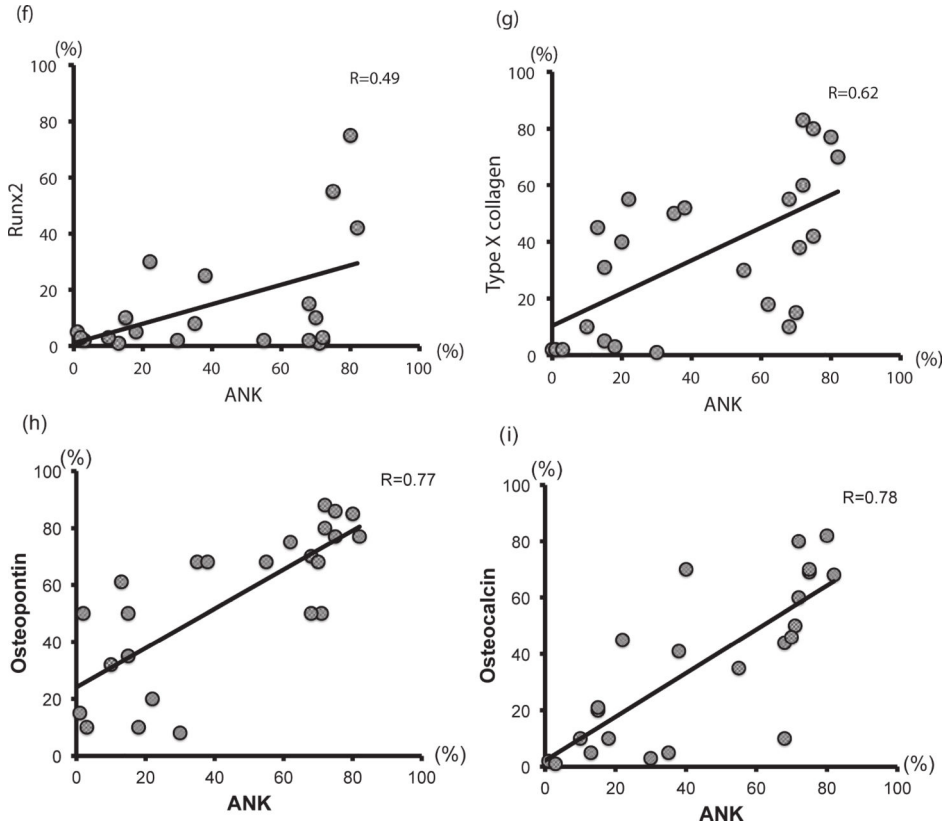

Figure 6F-I.

The number of ANK-positive cells significantly correlated with that of (f) Runx2, (g) type X collagen, (h) OPN, and (i) OCN-positive cells (r = 0.49, r = 0.62, r = 0.77, r = 0.78, respectively).

Table 1

Summary of the number of ANK-positive cells in immunohistochemistry. A. The total number of cells and number of ANK-positive cells were counted in at least 20 different microscopic high-power fields (HPF; x 400) chosen randomly from each section. B. The results were expressed as the positive ratio (positive cells/number of total cells) x 100 (%) at a magnification of x 400. ANK positivity in the extracellular matrix was measured by calculating [positive area of matrix/total area of matrix] x 100 (%).

A	**Healthy, n = 6** **mean ± SD (range)**	**OA, n = 11** **mean ± SD (range)**	**CPPD, n = 24** **mean ± SD (range)**
Cartilage			
Total cell number	27.3 ± 8.3 (17–40)	42.2 ± 17.8 (29–68)	47.6 ± 22.1 (20–74)
Cytoplasm	0.27 ± 0.45 (0–2)	15.1 ± 3.04 (9–30)	29.8 ± 7.04 * (8–59)
Membrane	0 (0–0)	3.84 ± 1.01 (2–8)	24.56 ± 6.66 * (5–50)
Meniscus			
Total cell number	45.1 ± 16.9 (22–60)	41.4 ± 12.0 (28–56)	53.7 ± 16.3 (41–72)
Cytoplasm	0.23 ± 0.09 (0–2)	16.56 ± 4.6 (6–29)	41.8 ± 7.84 * (15–56)
Membrane	0 (0–0)	0.66 ± 0.33 (0–2)	36.1 ± 10.7 * (13–52)
Synovium			
Total cell number	33.1 ± 10.6 (22–45)	45.3 ± 13.1 (36–60)	47.5 ± 10.2 (38–62)
Cytoplasm	0.13 ± 0.03 (0–2)	3.76 ± 2.40 (2–11)	27.4 ± 10.9 * (6–44)
Membrane	0 (0–0)	0.082 ± 0.1 (0–2)	19.9 ± 7.65 * (5–39)
B	Healthy, n = 6 mean ± SD (range)	OA, n = 11 mean ± SD (range)	CPPD, n = 24 mean ± SD (range)
Cartilage (%)			
Cytoplasm	1 ± 1.65 (0–4.3)	35.7 ± 7.2 (26.5–48.2)	62.6 ± 14.8 * (38.8–93.2)
Membrane	0 (0–0)	9.1 ± 2.4 (5.5–13.1)	51.6 ± 14.0 * (18.1–73.4)
Matrix	0 (0–0)	12.4 ± 4.2 (6.4–19.4)	54.8 ± 12.7 * (30.2–70.4)
Meniscus (%)			
Cytoplasm	0.5 ± 0.2 (0–0.6)	40.0 ± 11.1 (20.5–55.8)	77.9 ± 14.6 * (31.8–91.1)
Membrane	0 (0–0)	1.6 ± 0.8 (0–5.1)	67.2 ± 19.9 * (28.2–85.9)

A	Healthy, n = 6 mean ± SD (range)	OA, n = 11 mean ± SD (range)	CPPD, n = 24 mean ± SD (range)
Matrix	0 (0–0)	11.4 ± 2.7 (6.9 –16.4)	64.6 ± 22.3 * (38.4–80.1)
Synovium (%)			
Cytoplasm	0.4 ± 0.1 (0–0.5)	8.3 ± 5.3 (3.1–20.4)	57.7 ± 23.0 * (11.8–79.5)
Membrane	0 (0–0)	0.18 ± 0.22 (0–0.7)	41.9 ± 16.1 * (10.5–70.5)
Matrix	0 (0–0)	1.68 ± 1.41 (0–4.1)	22.3 ± 7.5 * (9.4–40.2)

* $p < 0.001$ vs OA and control. OA: osteoarthritis; CPPD: calcium pyrophosphate dehydrate.